Journal of Energy Storage 56 (2022) 105966

Contents lists available at ScienceDirect

Journal of Energy Storage

journal homepage: www.elsevier.com/locate/est

Research papers

Pumped heat energy storage with liquid media: Thermodynamic assessment by a transcritical Rankine-like model

D. Salomone-González [a], P.L. Curto-Risso [a], A. Calvo Hernández [b,c], A. Medina [b,c], J.M.M. Roco [b,c], J. Gonzalez-Ayala [b,*]

[a] Facultad de Ingeniería, Universidad de la República, Montevideo, Uruguay
[b] Instituto Universitario de Física Fundamental y Matemáticas (IUFFyM), Universidad de Salamanca, 37008 Salamanca, Spain
[c] Departamento de Física Aplicada, Universidad de Salamanca, 37008 Salamanca, Spain

ARTICLE INFO

Keywords:
Energy storage
Water storage
Coupled transcritical Rankine model
Round trip efficiency
Internal and external irreversibilities
Heat leak

ABSTRACT

A pumped heat energy storage (PHES) system based on a Rankine cycle for supercritical working fluids, such as carbon dioxide and ammonia, accounting for the irreversible latent and sensible heat transfers between the working fluid and the storage liquid medium, as water or thermal oil, is analyzed. The model also includes several parameters such as pressure losses, heat exchanger efficiencies, and isentropic efficiencies of the compressor, pump, and expansion devices (such as turbines and valves), that take into account the main internal and external losses and heat leak to the environment. The model allows for the calculation of specific energy, the heat pump performance coefficient, heat engine efficiency, and overall round-trip efficiency, as well as the temperatures of the working fluid and reservoirs. A zero-dimensional model is also used to determine the time dependence of heat leak in the tanks. The main results show that this technology could achieve round trip efficiency values in the order of 50–70%. Irreversibilities in compression and expansion appears as the most influential energy losses factor. The time effect of the ambient conditions on the tanks has been analyzed for a wet subtropical climate but it seems that the ambient conditions have no major influence on the performance of the system. In addition, explicit numerical results and temperature–entropy plots are presented for two representative systems as carbon dioxide-water and ammonia-thermal oil to take into account the main values in an operating condition.

1. Introduction

To reduce emissions of CO_2, and surpass the increase in fuel prices and the more restrictive environmental regulations, the control of energy consumption becomes more and more important [1]. Along this line, it is essential to reduce the use of fossil fuels through electricity generation systems from renewable sources (wind, hydroelectric, photovoltaic, etc.). However, beyond the economic and environmental advantages, the production of electricity from renewable sources can be intermittent and difficult to control by the electric grid operators. In addition, it is important to point out that the energy consumption of the communities is usually quite regular, with high demand at certain times of the day which, in general, are non-coincident with the peaks in the renewable energy production [2].

According to the need to avoid these variations, without the use the fossil fuel power plants, it is appealing that the analysis of novel energy storage systems could improve the grid stability, increase the penetration of renewable energy resources, conserve fossil energy resources, and reduce the environmental impact of power generation. One kind of useful technology to achieve the above goals is based on the store of surplus electricity in the form of high temperature heat and power [3] employing a heat pump device (charge period) from where it is then extracted (discharge period) as electrical energy using a thermal heat engine when needed [4]. This technology can be used not only for electricity storage/production but also for cogeneration of electricity and heat or even trigeneration of electricity, heat, and cold. In [5], a detailed description and fundamentals of the system and how it works are presented. Currently, there have been few experiences in thermal storage. In 2014 in Germany, a small-scale pilot plant was installed in Hamburg Bergedorf [6] with a storage capacity of 5 MWh where various storage concepts, materials, and assemblies were tested. Then, it was upgraded to a capacity of 130 MWh stored in volcanic rocks that were connected to the Hamburg grid in June 2019. Also,

* Corresponding author.
E-mail addresses: danielsalomonegonzalez@gmail.com (D. Salomone-González), pcurto@fing.edu.uy (P.L. Curto-Risso), anca@usal.es (A. Calvo Hernández), jgonzalezayala@usal.es (J. Gonzalez-Ayala).

https://doi.org/10.1016/j.est.2022.105966
Received 23 June 2022; Received in revised form 20 September 2022; Accepted 23 October 2022
Available online 5 November 2022

Nomenclature

c_p	Specific heat (J/kg K)
C	Heat capacity (W/K)
D	Diameter (m)
e	Thickness (m)
h	Enthalpy (J/kg)
M	Mass (kg)
$\dot{m}$	Mass flow (kg/s)
P	Pressure (MPa)
Q	Heat (W)
r	Pressure ratio
t	Time (h)
T	Temperature (K)
W	Work (W)
x	Cycle ratio = r^{HP}/r^{HE}
COP	Coefficient of performance
$PHES$	Pumped heat energy storage
PP	Pinch point
RTE	Round trip efficiency

Greek letters

ε_i	Efficiencies
γ	Adiabatic coefficient
Γ	Heat capacity ratio
η	Heat engine efficiency
ξ	Heat leak coefficient

Subscript

c	Compressor
$crit$	Critical
H	High pressure zone
HE	Heat engine
HP	Heat pump
L	Low pressure zone
min	Minimum
p	Pump
t	Turbine
w	Working fluid
0	Ambient
1-4	Points of the cycle

there are currently several projects around the world to build the first series of commercial pilot plants in a range of 10 to 100 MW ranging from a combination of packed bed tanks and different kinds of cycles to supplementary organic Rankine cycles tested by researchers in Denmark [3,4], resulting in a power-to-power efficiency of about 30%.

Nowadays, a specific technology for electricity storage at large- and medium-scale applications appears inspired by some of the projects mentioned above. Pumped heat energy storage (PHES) systems usually work with a single-phase working gas operating in a round-trip Brayton-like cycle or a fluid operating on round-trip Rankine-like cycles with appropriate solid or liquid components as storage systems. Sensible packed-bed materials, due to their wide temperature range, high efficiency, and small pressure losses [7] have been studied for large-scale electric applications [8], using thermodynamic analysis [9] with main internal and external losses [10], parametric optimization [11] and response to cycle duration perturbations [12]. Guo et al. [13] developed a finite-time numerical model to estimate the system performance, obtaining values in the order of 20%–40% global efficiency. Optimization algorithms, providing trade-off surfaces (Pareto fronts) from which insights on how the optimal design (Pareto optimal sets) should vary when multiple objectives are considered, have been also reported [14].

The main Brayton PHES studies were done on solid storage, but also high-temperature fluids have been used as storage media for the heat treatment industry and in concentrated solar power plants (i.e. solar towers) [15]. Also, some companies are beginning to develop pilot plants with inexpensive components and raw materials because much of the system uses conventional and easy-to-procure technology like steel tanks, air as a working fluid, and cooling liquids like water [16]. Some researchers like Laughlin [17], Farres et al. [18] or Salomone et al. [19,20] studied solar salts and thermal oils for high-temperature reservoirs and cold fluids like methanol and hexane with reported round trip efficiencies in between 20 and 40% under normal operating conditions.

The transcritical Rankine-like cycle has recently been proposed for pumped heat energy storage (PHES) technology due to its versatility for working on subcritical, supercritical and/or transcritical fluid conditions. The technology is promising since thermal energy can be stored in tanks at a relatively low cost and generally presents a high energy density, especially due to the use of latent heat storage, even though the necessary high pressure levels imply the use of more demanding compression machines and consequently, a higher initial investment cost [21].

The first studies on PHES technology with Rankine cycle were carried out by Hemrle and Mercangöz [22]. They presented a system using transcritical CO_2. Additionally, Morandin and Maréchal [23], seeking the improvement of the transcritical technology, developed a procedure based on empirical curves obtained by Hemrle [22] and optimized the thermal integration between the charge and discharge cycles. Inspired by this work, a preheater was included before the compressor in the charge period, which allowed the increasing in the temperature of the hot tank and thus the power produced at discharge [24,25]. Finally, based on suppliers prices, they developed an economic model where the impact of the high cost of high pressure cycles and the number of intermediate reservoirs was recognized [26]. Later, Kim et al. [27] (based on the Hemrle and Mercangöz work) studied the application of an isothermal model and made modifications to the compression and expansion stage to optimize the global round trip efficiency (RTE). These studies led Fauci et al. [28] to study the construction of a 5 MW PHES pilot plant in Zurich. The proposed working fluid was CO_2, operating between 30 and 140 bar with storage temperature of the hot reservoir of 120 °C and the cold one, 0 °C. To improve the overall system efficiency, they proposed a possible integration of the PHES with the district heating system. The use of other refrigerants such as ammonia, is just beginning to be studied by the academic community, by Koen et al. [29] or Abbar et al. [30]. They use storage media other than water to develop the transcritical Rankine technology. For instance, Koen uses thermal oils (such as Therminol DS12 and 66) to reach the temperatures needed for ammonia while Abarr works with a novel concrete tube exchanger. Moreover, recently, Zhao et al. [31] presents three different variants of the pumped thermal electricity storage system (PHES) based on currently available sensible heat storages and one of them is transcritical Rankine with different thermal oils and pressurized water.

In regards to compression and expansion devices, transcritical cycles have several advantages compared to those using Brayton cycles with working fluids in a gaseous state. This occurs due to the compression of the working fluid during discharge in the liquid region, where its density is high enough to use simple pumps instead of compressors, thus reducing the compression work and increasing the generated power. Additionally, in this region, the supercritical fluid behaves like a liquid in terms of compressibility and heat transfer characteristics allowing more efficient heat exchange. In short, machines and heat exchangers will be smaller [27].

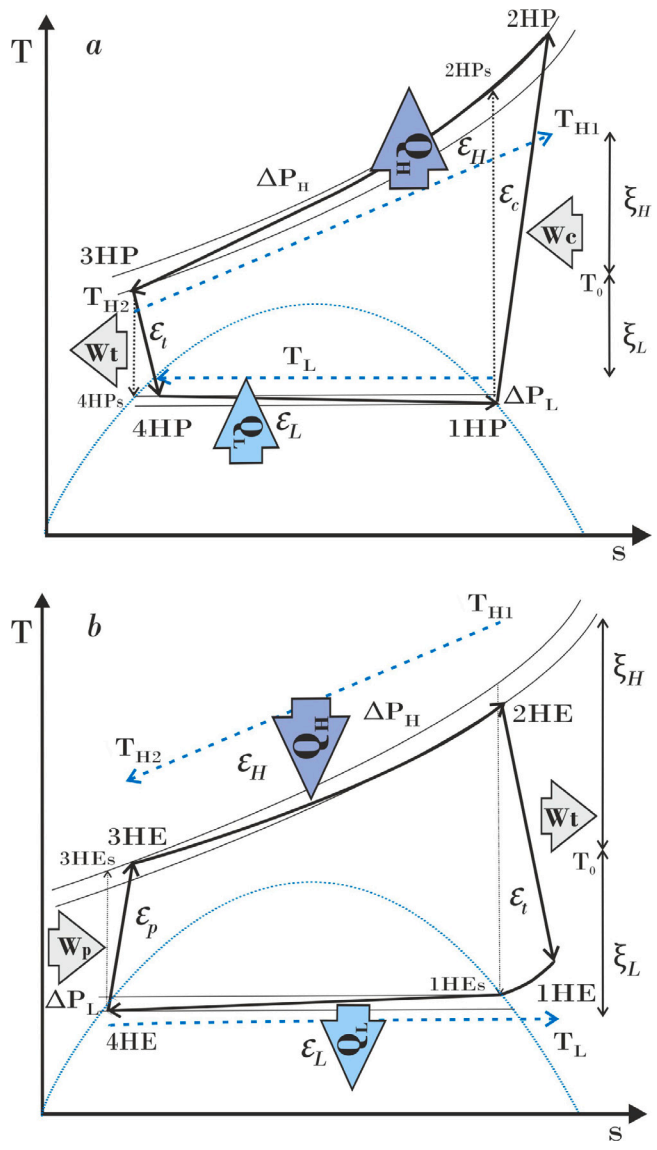

Fig. 1. Transcritical Rankine cycle with irreversibilities for PHES (a) *Heat pump (HP)* – Composed of an isentropic compression (1HP-2HP), a high temperature heat exchange (2HP-3HP), an isenthalpic or isentropic expansion (3HP-4HP) and a low temperature heat exchange (4HP-1HP) and (b) *Heat engine (HE)* – Composed of an isentropic compression (4HE-3HE), a high temperature heat exchange (3HE-2HE), an isentropic expansion (2HE-1HE) and a low temperature heat exchange (1HE-4HE). ε represents the efficiencies of the equipment, ΔP the pressure drops and ξ the heat leak. Details on all these parameters are given in Section 4.

The main purpose of this work is to model this specific energy storage technology, to analyze its main variables and capabilities with a detailed analysis of the different involved irreversibilities. Therefore, the proposed model takes into account the description of the charge and discharge modes and their coupling. It includes the internal losses of the compressors, pumps and expanders (turbine, valves or hydraulic expanders), the pressure drops of the working fluid, the heat leak to the environment and the external coupling of the working fluid with the cold and hot storage liquids. The model allows to obtain explicit analytical and numerical results for the main energetic metrics such as the efficiency (η) of the HE cycle, the coefficient of performance (COP) of the HP cycle and the round-trip efficiency (RTE) of the overall device in terms of the losses considered. From this, an additional advantage of the model is its ability to test parametric optimization and design strategies based on a reduced set of parameters that take into account hot and cold tanks, and the charging and discharging power blocks. In summary, it constitutes a complete thermodynamic description of the main processes and their interaction for a selected layout without the high computational costs of dynamic models.

The paper is structured as follows. Section 2 contains the analysis of the working fluids and hot and cold liquids that will be used along the paper. Section 3 contains the description of the HE and HP cycles, their coupling, and the overall thermodynamic model, including the main involved losses. Section 4 contains the numerical results and some discussions of HE efficiency, HP coefficient of performance and overall round-trip efficiency for the system using CO_2 and water and with particular emphasis on the influence of internal and external losses. For the same case, the heat leak to the environment is analyzed over time to estimate how the reduction in efficiency is affected. Additionally, particular examples (for systems with CO_2 and NH_3) are also presented to explicitly show the individual T–s behaviors for HE and HP cycles, as well as to calculate specific values of the corresponding efficiency η, COP and round-trip efficiency RTE. Finally, in Section 5, the main conclusions and some perspectives are presented.

2. System description

The temperature–entropy (T–s) sketches for heat pump and heat engine of the simplest transcritical Rankine cycle in a PHES system are presented in Fig. 1 while the overall arrangement is presented in Fig. 2. The shape of the diagrams, very different from that of the Brayton cycle (the other usual arrangement used for PHES with liquid storage), is due to the different type of heat exchange in the low and high pressure zones of the cycle.

The main feature of this type of cycle is that on the cold tank side, heat exchange takes place at a constant temperature with the working fluid under the saturation curve while on the high-pressure side the working fluid undergoes heat exchange in a supercritical process without any phase change and therefore with a variable temperature profile [32,33]. Accordingly, the charging system, the HP-cycle, includes a work recovering expander, an evaporator, a compressor, and heat exchangers, and the discharging system, the HE cycle, includes a liquid pump, a condenser, a CO_2 turbine, and heat exchangers. As storage systems, water in the hot reservoir and ice slurry in the cold one were used. The storage system includes a heat exchanger with a circuit for the working fluid where a transcritical process happens during heat transfer. The circuit has a hot storage tank, an intermediate temperature tank, and a cold storage tank connected via the heat exchanger. One interesting feature is that a decrease in the temperature of the cold source by using ice is more favorable in the obtained efficiency than an increase in the high temperature of the hot tank.

2.1. Supercritical working fluids

A supercritical fluid is a substance that works above its critical temperature (T_{crit}) and critical pressure (P_{crit}). These fluids are interesting in their utilities since they adopt properties intermediate between liquids and gases (densities, diffusion coefficients and viscosities). Their transport properties are close to those of gases: low viscosity, high diffusivity, very low surface tension, and similar solvating power to that of liquids. Their high compressibility makes it possible to manipulate and modify their density and solvating power, making them similar to liquids or gases, depending on their application [34].

Table 1 shows critical values, formulas and safety levels (SL) for some working fluids.[1] Preferably, the working fluid of a PHES system should be safe to handle. However, few fluids are completely harmless, so the question is what constitutes an acceptable risk to the industry.

[1] Safety levels in the ANSI/ASHRAE 15-1992, refrigerants are classified according to the danger involved in their use. Group A1 refrigerants are the least dangerous and group B3 refrigerants are the most dangerous.

Table 1
Critical values (T_{crit} and P_{crit}), formulas and safety levels (SL) for different common refrigerants [35].

Refrigerant	N°	Form.	T_{crit} (°C)	P_{crit} (MPa)	SL
Carbon dioxide	R744	CO_2	31.1	7.38	A1
Water	R718	H_2O	376.9	2.21	A1
Ammonia	R717	NH_3	132.9	11.2	B2
Butane	R600	C_4H_{10}	152.0	3.8	A3
Sulfur dioxide	R764	SO_2	157.5	7.9	B1

Therefore CO_2 is an attractive option for use as a working fluid in Rankine-type PHES due to its good thermo-physical properties, such as its low critical point and high power density. It is non-toxic, non-flammable, safe (A1), compatible with standard materials and lubricants and it is a natural refrigerant with low global warming potential. In addition, the very low dynamic viscosity and high density of CO_2 result in good heat transfer coefficients, so that large transfer rates are achieved with relatively small surface areas. Another advantage of CO_2, especially for the charging stage of the PHES system, is that it has a low surface tension, which reduces cavitation effects in the machinery and allows compression and expansion closer to the saturation curve [26,36]. From an economic point of view, its price is up to ten times lower than R22 or an half the cost of ammonia (NH_3-R717).

Since the critical point of CO_2 occurs at a low temperature, it should be careful that the fluid conditions do not reach the triple point (−57 °C and 0.52 MPa) [37]. If the system is not properly designed and controlled, a solid, liquid and gaseous states can coexist, which is a limitation on the operating temperatures.

The disadvantage is that it is an asphyxiating gas and requires high pressures to reach moderate temperatures [32]. Another drawback of transcritical carbon dioxide is the larger pressure required to reach reasonable temperatures, given the lower adiabatic coefficient of expansion ($\gamma = 1.3$) with respect to that of Argon ($\gamma = 1.67$) or air ($\gamma = 1.4$). Values reported in the literature about transcritical Rankine CO_2-PHES systems show working pressures of 150 to 200 bar in the high temperature zone [32]. This must be considered in the design of piping and heat exchangers. Another important issue is that the maximum pressure that compressors can reach is about 200 bar (a high but reasonable technical–economic limit), therefore a significant size is required to operate at maximum temperatures close to those obtained with air or Argon compressors [38].

The work of Aga et al. [39] provides some hints on the needed characteristics of the turbomachinery. It takes as its main restriction the high pressures required by the compressors and they use only machinery and technology present in the market at the date of publication of their article and not those still under development. They use a Brayton CO_2 model focusing on the restrictions to reaching high temperature and pressure. In this way, it presents a proposal based on a compressor and expander from the oil and gas industries. In practice, this implies that the compressor is limited to a maximum, and to reach the temperature of ideal storage of molten salts, it is necessary to supplement with an electric heater, which reduces the efficiency of the charge cycle but benefits the overall performance of the system. This can be an alternative option when it is preferred to reduce the operating pressure ratios but at the cost of lower efficiency.

Recently, Koen et al. [29] and Abbar et al. [30] have studied the use of ammonia. Ammonia as a working fluid has good thermodynamic properties for transcritical Rankine PHES. It has an elevated critical point (see Table 1), which implies a more demanding compressor (higher critical points values imply higher pressure ratios), but on the other hand it has a lower triple point (−78 °C and 6.06×10^{-3} MPa), therefore it can be worked at lower pressure levels than CO_2. Although ammonia has inherent risks due to its toxicity and flammability (B2), it is very commonly used on an industrial scale.

2.2. Storage fluids

Regarding energy storage, the current literature focuses on both packed-bed reservoir systems and two-reservoir systems with thermal fluids (salts or liquid metals). In the case of Rankine cycles, it should be clarified that the main trend is towards the use of pressurized water or thermal oil as storage medium, operating with a brine ice suspension for the cold reservoir. Considering the practical benefit when the working fluid and storage fluid are both under two-phase conditions, the transcritical cycle is suitable to operate with a constant temperature reservoir (and a variable temperature reservoir on the high pressure side). Therefore, the use of oils or pressurized water (in the high temperature zone) and ice water (in the low temperature zone), seems to be an option of interest that has been studied by several authors [22,24,32].

2.2.1. Hot storage fluids

Hot water thermal storage is very used, since has high thermal capacities (and consequently high energy density, in both volume and mass, compared to molten salts or solids), is harmless (as it is non-flammable, non-toxic and non-corrosive), is naturally available, is environmentally friendly and, moreover, it has a low price. It also has excellent heat transfer and heat transport properties. An additional advantage is that, by working at lower temperatures than Brayton cycles, losses to the coldest parts of the plant (heat leak) will be lower. This feature improves the long-term liquid storage possibilities. The maximum storage temperature is limited by the boiling temperature but these temperature levels in the hot reservoir can be raised by using pressurized tanks or by adding some salts to increase its boiling point [40].

Other alternative fluids in the hot reservoir, such as thermal oils, provide a low or medium range of possible storage temperatures (in the range between −115 °C and 400 °C) for Rankine cycles, especially when ammonia is used as working fluid, whose critical point is above 130 °C. The fluid, unlike molten salts, is pumpable at low temperatures and offers high-temperature thermal stability [29].

2.2.2. Cold storage fluids

In the cold reservoir, the constant temperature value due to the phase change in the heat exchanger suggests that it would be a good option to use the latent heat obtained from an ice suspension in a dilution of antifreeze (ice slurry or liquid ice) or an ice bank. The most economical, but less efficient option may be the use of a relatively constant temperature source such as the ground or ambient air. It should be mentioned that having an ice water storage should not disregard the possibility of using in series an external heat reservoir (air, water, ground) to discharge part of the energy that cannot be converted. Other storage media could also be used, such as alcohols and hydrocarbons from Brayton cycles, but the features of constant temperature and reduced cost of ice water in the low temperature zone seems to be a good choice for this case. Although liquid ice has great and diverse advantages, the density and enthalpy gradient make the reservoir volumes larger compared to the use of other cryogenic fluids such as methanol or hexane.

Liquid ice is a technology under strong development because of its high potential within the refrigeration industry in order to get increasingly efficient and environmental friendly systems. It consists of a suspension of microcrystals in an aqueous solution, which allows the freezing temperature of the solution to be reduced below that pure water. While pure water crystallizes only at 0 °C and can be used to generate liquid ice, a mixture of salt water with calcium or sodium chloride or other antifreeze agent (glycols, such as ethylene glycol or propylene glycol and alcohols, such as ethanol or propanol) can be considered to explore the option of cold storage at lower temperatures. The simplest and most economical is the use of sodium chloride (NaCl). The phase change of NaCl and water mixtures can be obtained between

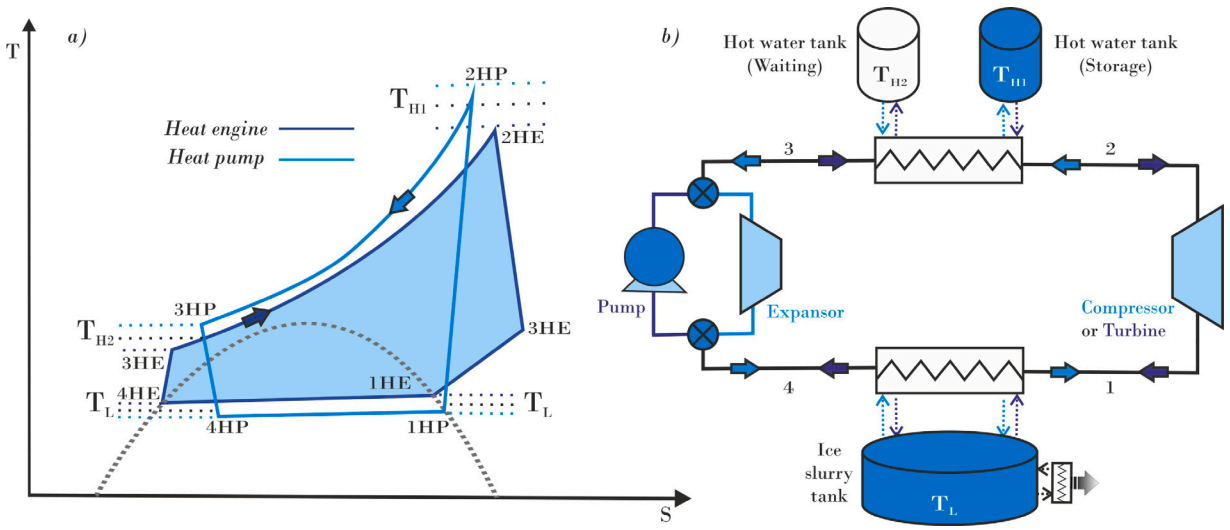

Fig. 2. Transcritical Rankine for PHES. Combined cycles: (a) heat engine (dark blue) and heat pump (light blue); (b) scheme of the corresponding components. (For interpretation of the references to color in this figure legend, the reader is referred to the web version of this article.)

0 °C and −21.2 °C [41]. Cold storage is then obtained by freezing the brine and a remnant of suspended solid ice will remain in the tanks [26].

The ice fraction defines the melting point, the properties of the liquid and, for the purposes of fluid transport, this value cannot exceed 30%. As there is more solid ice, there will be more antifreeze in the liquid and the freezing point temperature is reduced to a minimum where the concentration is reached where the salt and water form a eutectic solution (about−21.5 °C) and then starts to rise [42]. The heat exchanged in relation to the freezing process for the PHES low reservoir can be calculated by enthalpy diagrams. In this work it is used Coolprop [43] for fluids properties. For the case of brine the physical properties presented by Melinder [42] are used.

In summary, the use of water as storage medium in reservoirs requires a thermal cycle that can operate with low temperature heat, so CO_2 is chosen in a transcritical process to optimally match the thermal profiles of the working fluid and the water used as storage medium [44]. On the other hand, the critical conditions of NH_3 do not allow the use of water in the storage tanks, so the system uses thermal oils that resist higher temperatures and remain liquid in the operating range.

3. Method

The proposed overall arrangement consists in a combination of a Transcritical Rankine-like HP cycle followed by a Transcritical Rankine-like HE cycle.

3.1. Heat pump cycle

The heat pump Rankine cycle for the charge mode, see Fig. 1a, shows, in addition to the different equipment and relevant points of the cycle, the main type of involved irreversibilities: the external irreversibilities are due to the finite temperature difference between the system and external reservoirs and heat leak, while the internal irreversibilities are due to pressure drops due to friction in pipes and heat exchangers and entropy generation in compressors, pumps and turbines.

In relation to Fig. 1a, the HP cycle starts with an irreversible mechanical compression W_c with isentropic efficiency ε_c that raises the temperature of the working fluid from T_1^{HP} to T_2^{HP}. The hot gas reaches a supercritical state and it is used to irreversibly heat up the storage liquid (with an efficiency of ε_H) from T_{H2} to T_{H1} in the high temperature reservoir through process $2HP \rightarrow 3HP$. The temperature of the fluid drops from T_2^{HP} to T_3^{HP} and the pressure is slightly reduced due to frictional losses with a drop of ΔP_H. This cooling process of the working fluid under supercritical conditions does not lead at any time a phase change. Next step is an irreversible expansion W_t (with isentropic efficiency ε_t) along the $3HP \rightarrow 4HP$ process take place. In order to increase the RTE, a hydraulic expander can be used to recover the expansion work on the liquid zone of the cycle instead of an expansion valve, although this clearly involves higher cost. Expansion valves are generally used in heat pump and refrigeration cycle designs for liquid expansion at the condenser outlet as a simple, practical and low-cost component. In the case of PHES, a liquid expander can recover some work and improve the cycle efficiency. If the system uses an expansion valve at this point instead of a recovery expander, the expansion becomes an isenthalpic process in which all the power that could be recovered is lost. In this paper, where the aim is to establish situations as close to reality as possible, expansion valves will be used since they are easily found in the market. Then, in the expansion process, the temperature and pressure drop from $T_3^{HP}(P_3^{HP})$ to $T_4^{HP}(P_4^{HP})$ and the fluid is in a liquid state under subcritical conditions. Finally, in the process $4HP \rightarrow 1HP$ the working fluid undergoes a phase change (it evaporates) driven by the addition of heat coming from the low temperature reservoir where T_{L2} reduced to T_{L1} or, if ice water is used as in Fig. 1a, a phase change occurs at constant temperature but with a pressure drop ΔP_L. At this stage, during the addition of heat from the cold reservoir, the fluid remains at a nearly constant temperature. In such a situation of change of state, the working fluid could be in different phases. For example, it can be subcooled liquid, saturated liquid, a liquid–vapor mixture, saturated vapor or even superheated vapor (towards the end of the evaporation process) [45,46].

To account for the inherent irreversibilities, isentropic and heat exchange efficiencies, pressure drops and heat leak are defined below. Since there are phase changes, enthalpy values are considered for each working fluid and storage media.

3.1.1. Pressure losses

Due to frictional effects in the fluid flowing through the heat exchangers and pipes connecting the components, pressure drops must be considered. These effects are expected to be more significant in liquids than in gases due to their viscosity and density values. In fact, pressure losses in most of the studies in the literature are neglected; here, the proposed model includes both a ΔP_H loss of the supercritical

fluid flowing through the high pressure heat exchanger and a ΔP_L loss for the low pressure side, quantified as:

$$\Delta P_H^{HP} = P_2^{HP} - P_3^{HP} \quad \text{and} \quad \Delta P_L^{HP} = P_4^{HP} - P_1^{HP} \tag{1}$$

3.1.2. Irreversibilities in expansion and compression

Assuming a nonadiabatic operation for the compressor and turbine, the model uses the common isentropic efficiency equations defined by the enthalpies.

For the compressor:

$$\varepsilon_c = \frac{h_{2s}^{HP} - h_1^{HP}}{h_2^{HP} - h_1^{HP}} \quad \text{so} \quad h_2^{HP} = \frac{h_{2s}^{HP} - h_1^{HP}}{\varepsilon_c} + h_1^{HP} \tag{2}$$

For the expander:

$$\varepsilon_t = \frac{h_3^{HP} - h_4^{HP}}{h_3^{HP} - h_{4s}^{HP}} \quad \text{so} \quad h_4^{HP} = h_3^{HP} - \left(h_3^{HP} - h_{4s}^{HP}\right)\varepsilon_t \tag{3}$$

Therefore, the compressor and hydraulic turbine works are given, respectively, by:

$$W_c^{HP} = \dot{m}_w \left(h_2^{HP} - h_1^{HP}\right) = \frac{\dot{m}_w}{\varepsilon_c}\left(h_{2s}^{HP} - h_1^{HP}\right) \tag{4}$$

$$W_t^{HP} = \dot{m}_w \left(h_3^{HP} - h_4^{HP}\right) = \dot{m}_w \varepsilon_t \left(h_3^{HP} - h_{4s}^{HP}\right) \tag{5}$$

where h (h_s) stands for the specific enthalpy (isentropic conditions) and $\dot{m}_w$ the mass flow rate of the working fluid.

If the HP-cycle operates with a valve instead of a hydraulic turbine, the expansion is modeled as an isentropic throttling process where $h_3^{HP} = h_4^{HP}$. The pressure decreases on expansion and is accompanied by an increase in entropy. The fluid leaves the valve in state 4 as a two-phase liquid–vapor mixture. The net work of the cycle is equivalent to $W^{HP} = W_c^{HP} - W_t^{HP}$ and if using an expander valve is $W^{HP} = W_c^{HP}$.

3.1.3. Heat exchangers losses

During charging process, part of the heat from working fluid is taken from the cold reservoir. Then, as the fluid is compressed, its temperature is further raised up and finally transfers that energy to the storage system where it will be retained until discharge. In the high temperature heat exchanger the working fluid flows into the tubes and the storage liquid flows through the shell side. Both pass through the heat exchanger without changing phase.

The energy balance $\dot{Q}_H$ for the heat exchanged with the hot tanks shows that:

$$\begin{aligned}\dot{Q}_H^{HP} &= \dot{m}_w \left(h_2^{HP} - h_3^{HP}\right) = C_w \left(T_2^{HP} - T_3^{HP}\right) = \\ & C_H^{HP}\left(T_{H1}^{HP} - T_{H2}^{HP}\right) = C_{H,min}^{HP}\varepsilon_H^{HP}\left(T_2^{HP} - T_{H2}^{HP}\right)\end{aligned} \tag{6}$$

where C_H and C_w are the average heat capacities of the storage liquid and working fluid, respectively, ε_H^{HP} the effectivenesses of the hot heat exchanger, and $C_{H,min}^{HP}$ is the minimum value between C_H and C_w.

In the cold reservoir case, both fluids are changing phase, so there is no temperature variation as in the high reservoir. In this case, it should be understood that the thermal capacity of both fluids will be very high and cannot be evaluated in the same way as for the case of the high temperature zone. Therefore, this energy balance should be:

$$\dot{Q}_L^{HP} = \dot{m}_w \left(h_1^{HP} - h_4^{HP}\right) = \varepsilon_L^{HP}\dot{m}_L \left(h_{L2}^{HP} - h_{L1}^{HP}\right) \tag{7}$$

where ε_L^{HP} is the effectivenesses of the cold heat exchanger.

The model assumes, in addition to a low temperature exchanger efficiency (ε_L), a minimum temperature difference between the working fluid and the cryogenic fluid (ΔT_L^{HP}) to account for pinch point effects such that:

$$T_4^{HP} = T_L^{HP} - \Delta T_L^{HP} \tag{8}$$

3.2. Heat engine cycle

The Rankine cycle for the discharge (heat engine) is shown in Fig. 1b. As in the heat pump cycle, the Rankine heat engine system operates in a transcritical cycle with heat absorption above the critical point on the hot zone and below subcritical conditions on the low pressure zone.

At peak consumption hours, the system is discharged such that the working fluid is compressed from a saturated liquid situation using a pump with an isentropic efficiency (ε_p). The temperature and pressure rise from $T_4^{HE}(P_4^{HE})$ to $T_3^{HE}(P_3^{HE})$. At the pump outlet the fluid in supercritical condition reaches the maximum pressure and pass through the high temperature heat exchanger with a pressure drop ΔP_H^{HE}, that heat the fluid from T_3^{HE} to T_2^{HE} while the liquid stored reduces its temperature from T_{H1} to T_{H2}. After the heat exchanger, the fluid expanded in a turbine, with an isentropic efficiency ε_t, reducing its temperature and pressure to $T_1^{HE}(P_1^{HE})$ to obtain the energy that is transmitted to the electrical network. Later, the working fluid discharges its remaining energy into the cold tank, condensing along process $1HE \rightarrow 4HE$. The ice slurry thaws at approximately constant temperature by receiving heat from the working fluid, which lowers its temperature from T_1^{HE} to T_4^{HE} and then remains in a phase change situation until restarting the cycle with a net pressure drop ΔP_L. Temperatures may vary slightly due to pressure drop.

The losses for the case of the heat engine are presented below:

3.2.1. Pressure losses

In this case, pressure drops result:

$$\Delta P_H^{HE} = P_3^{HE} - P_2^{HE} \quad \text{and} \quad \Delta P_L^{HE} = P_1^{HE} - P_4^{HE} \tag{9}$$

3.2.2. Irreversibilities in expansion and compression

The isentropic efficiency for the pump and the turbine can be calculated from the enthalpies as follows.

For the pump:

$$\varepsilon_p = \frac{h_{3s}^{HE} - h_4^{HE}}{h_3^{HE} - h_4^{HE}} \quad \text{so} \quad h_3^{HE} = \frac{h_{3s}^{HE} - h_4^{HE}}{\varepsilon_p} + h_4^{HE} \tag{10}$$

For the turbine:

$$\varepsilon_t = \frac{h_2^{HE} - h_1^{HE}}{h_2^{HE} - h_{1s}^{HE}} \quad \text{so} \quad h_1^{HE} = h_2^{HE} - \varepsilon_t \left(h_2^{HE} - h_{1s}^{HE}\right) \tag{11}$$

Therefore, the equivalent work for the pump:

$$W_p^{HE} = \dot{m}_w \left(h_3^{HE} - h_4^{HE}\right) = \frac{\dot{m}_w}{\varepsilon_p}\left(h_{3s}^{HE} - h_4^{HE}\right) \tag{12}$$

In addition, for the turbine:

$$W_t^{HE} = \dot{m}_w \left(h_2^{HE} - h_1^{HE}\right) = \dot{m}_w \varepsilon_t \left(h_2^{HE} - h_{1s}^{HE}\right) \tag{13}$$

Therefore, the net work of the cycle is calculated by $W^{HE} = W_t^{HE} - W_p^{HE}$.

3.2.3. Heat exchangers losses

The heat exchanged in the high temperature heat exchanger is:

$$\begin{aligned}\dot{Q}_H^{HE} &= \dot{m}_w \left(h_2^{HE} - h_3^{HE}\right) = C_w^{HE}\left(T_2^{HE} - T_3^{HE}\right) = \\ & C_H^{HE}\left(T_{H1}^{HE} - T_{H2}^{HE}\right) = C_{Hmin}^{HE}\varepsilon_H \left(T_{H1}^{HE} - T_3^{HE}\right)\end{aligned} \tag{14}$$

And the heat exchanged at low temperature is:

$$\dot{Q}_L^{HE} = \dot{m}_w \left(h_1^{HE} - h_4^{HE}\right) = \varepsilon_L \dot{m}_L \left(h_{L2} - h_{L1}\right) \tag{15}$$

And there will be a minimum temperature differential ΔT_L^{HE} to account for pinch point effects so that:

$$T_4^{HE} = T_L^{HE} + \Delta T_L^{HE} \tag{16}$$

In addition to the latent heat exchange, the system must cool sensitively from point 1HE to the phase change. It should be interesting

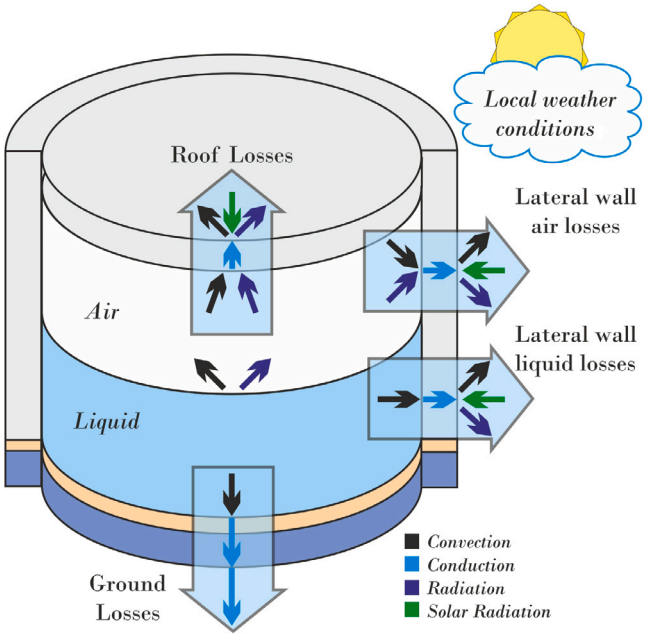

Fig. 3. Scheme of the tank with heat leak and the different involved heat transfer mechanisms [20].

that if the temperature T_1^{HE} is higher than ambient, this first section can be cooled with an exchanger with the surroundings temperature, but to be conservative in the analysis it will be assumed that all the gas in this stage lowers its temperature with the ice slurry.

3.3. Heat leak losses

Assuming a linear model of heat losses associated with the average ambient temperature, the heat leak equations affecting the high temperature storage tank can be written as:

$$T_{H1}^{HE} = T_{H1}^{HP} - \xi_H (T_{H1}^{HP} - T_0) \tag{17}$$

where ξ_H denotes an effective heat leak coefficient and T_0 the ambient temperature. The value of the coefficient ξ_H will depend on the ambient conditions and storage time and can be evaluated using a model of the heat transfer of the liquid within the tank and the ambient.

The calculation procedure and details for the heat leak coefficient is taken from Salomone et al. [20] where the net heat loss that cause hot liquid to cool can be subdivided into four main components: losses through the ground, the roof, the wall in contact with the air over the liquid and the wall in contact with the liquid. In each of these interfaces, the model develops all the mechanisms involved in convection, conduction, radiation and incident solar radiation. On the other hand, the model takes into account the local climatic conditions where the system is installed, so the calculations use factors such as ambient, ground and sky temperature, surrounding wind speed and incident solar irradiation (See Fig. 3 for a scheme of the tank, the involved heat leaks and different heat transfer mechanisms).

Here, the heat leak losses for the waiting tank (at T_{H2}) and cold reservoir (at T_L) will be considered negligible since the waiting tank temperature is close to ambient and insulation is not required. Thus, only heat leak from the tank at T_{H1} will be considered in this work.

3.4. Overall analysis

During the charging process, electricity is stored as potential thermal energy by increasing the temperature of the hot storage medium and lowering the temperature of cool storage medium, through the transcritical heat pump cycle. During the discharge, the stored thermal energy is converted back to electricity through the coupling of the HP and HE modes Rankine-type transcritical cycles. The overall arrangement is presented in Fig. 2.

To mimic a real behavior system, it is necessary to define some key restrictions for the involved temperatures of both the storage system and the working fluid. The liquid must remain in that state in the hot tank, so the temperature must be higher than the crystallization temperature (T_{crist}) and less than the boiling temperature (T_{boil}). In the cold tank, the temperature must always be below the level of the crystallization temperature. On the other side heat transfer processes between the working fluid and the tanks in the charge and discharge modes require a pinch point (PP) gradient. These restrictions are accounted for by the following conditions:

$$\begin{aligned} &T_2^{HE} + PP < T_{1HP} < T_2^{HP} - PP \\ &T_3^{HE} + PP < T_{2HP} < T_3^{HP} - PP \\ &T_{crist} < T_{2HP} < T_{1HP} < T_{boil} \\ &T_L < T_{crist} \end{aligned} \tag{18}$$

Since the initial temperatures at the beginning of each period should be fixed, it is very important to stabilize the system to get the right temperatures. In this line, at the outlet of the turbine in the discharge period, the fluid still has a high temperature and this energy must be removed to reach the inlet conditions in the charge period. Therefore, it must be additionally cooled with a refrigeration system to keep the temperature T_L constant.

The mass contained in the hot tank (M_H) and in the cold tank (M_L) will be given by:

$$M_H = \frac{\dot{m}_w c_{pw} t}{c_{pH} \Gamma_H} \quad \text{and} \quad M_L = \frac{\dot{m}_w (h_1 - h_4) t}{\varepsilon_L (h_{2L} - h_{1L})} \tag{19}$$

where c_{pw} and c_{pH} are the specific heats at the average temperature for the working fluid and the storage fluid, respectively. $\Gamma_H = m_w c_{pw} / m_H c_{pH} < 1$. t is the preset charging or discharging time. Γ_H and t values can be different in the HP cycle and the HE cycle, so the cycle that gives the highest mass in the storage tank is taken for the design.

The heat pump cycle coefficient of performance (COP), heat engine cycle efficiency (η_{HE}) and round trip efficiency (RTE) of the overall heat pump cycle system are quantified according to the model developed by Salomone et al. [19]. Definitions are as follows:

$$COP_{HP} = \frac{Q_H^{HP}}{W^{HP}} \quad \eta_{HE} = \frac{W^{HE}}{Q_H^{HE}} \quad RTE = \frac{\eta_{HE} Q_H^{HE}}{COP_{HP}^{-1} Q_H^{HP}} \tag{20}$$

4. Results and discussions

The following paragraphs present the results of a parametric study for the transcritical cycle using the model described above. An overall cycle ratio, $x = r^{HP}/r^{HE}$, associated with heat pump and heat engine pressure ratios is defined in order to fix the size ratio of both cycles and considering r^{HP} as the independent variable in the analysis.

Firstly, the transcritical system with carbon dioxide and water as storage medium is analyzed in detail, including the heat leak effects of the water tanks on the time evolution of the RTE. Next, and for sake of comparison, two particular configurations with CO_2-water and NH_3-thermal oil are presented, including numerical values of the main parameters and the corresponding $T - s$ plots.

4.1. Performance parametric evaluation

The theoretical model, including all described irreversibilities, was implemented in Octave [47] and the properties of pressurized water and dry CO_2 as working fluid are calculated with Coolprop [43] libraries, linked to Octave. The numerical results are obtained assuming that: (a) the compressor inlet pressure during the system charge (P_1^{HP})

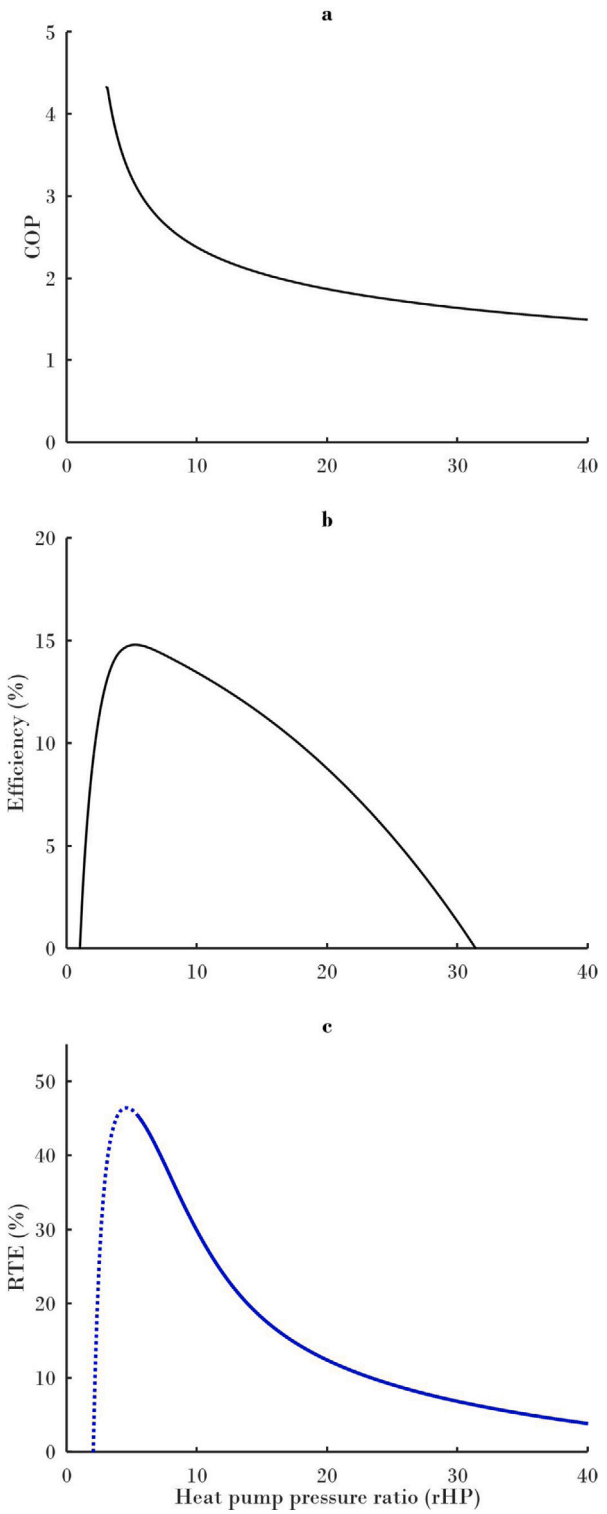

Fig. 4. (a) COP, (b) heat engine efficiency and (c) RTE as a function of pressure ratio r^{HP}. Baseline arrangement: $\varepsilon_c = \varepsilon_t = \varepsilon_p = 0.9$, $\varepsilon_H = \varepsilon_L = 0.90$, %ΔP = 1%, x = 2, P_1^{HP} = 2.5 MPa, ξ = 1%, ΔT_L = 5 °C, $T_{H2} = T_0$ = 17 °C, m_w = 100 kg/s. The dotted line represents the physically unavailable zones.

is equal to 2.5 MPa to ensure the liquid–gas phase change; (b) the pressure drop is equal in all heat exchangers and of the order of 1%; (c) the values of the efficiencies ε_c and ε_t in the compressors, expanders, valves and pumps are 0.90; and (d) the efficiencies of the high counterflow heat exchangers ε_H is 0.90, $x = 2$, a heat leak of (ξ) equal to 1.0% and a pinch point ΔT_L for the low temperature reservoir of 5 °C are also used. The temperature of the reservoir tank (T_{H2}^{HP}), before charging, is assumed equal to the average ambient temperature of the zone (T_0 = 17 °C for a humid subtropical climate).

In Fig. 4a the coefficient of performance (COP) for the heat pump is plotted in terms of pressure ratios r^{HP}. The COP shows a monotonic decreasing behavior with high values at low pressure ratios and then it becomes practically constant. Opposite, the efficiency of the heat engine and the overall RTE show a parabolic-like behavior with well defined peak values at different r^{HP}-values, between 5 and 7, as it can seen in Fig. 4b and c, respectively. Note that around the optimized pressure ratio, the values of the RTE are quite high in spite of that the corresponding COP and η values are moderate.

As mentioned above, in terms of operating temperatures some restrictions must be taken into account: firstly, to couple the power cycle with the heat pump cycle with a minimum required level of pinch point, and finally to keep the liquid nature of the water or thermal oil (see restrictions in Ec. (18)). Due to these constraints, in Fig. 4c not all values are thermodynamically accessible and the dotted lines correspond to the physically unavailable zone according to the restrictions on temperatures and the effects of the pinch point.

Efficiency and power output are two key magnitudes in the analysis of any heat engine. These magnitudes are usually obtained in terms of a set of independent variables and some control parameters. When in between these two magnitudes it is possible the elimination of the independent variables the resulting power-efficiency plots (usually loop-like) contains very useful information on their maximum values (close but non-coincident) for the remainder control parameters. In this analysis, such kind of plots can be easily obtained for the power output and RTE by the parametric elimination of the independent variable r^{HP} as can be seen in Figs. 5, 7 and 8 for different system parameters. Note that only the solid portion of each curve fits the restrictions on the temperatures and the effects of the pinch point given by Ec. (18).

Fig. 5a shows the loop-like behaviors of power versus RTE to gain information about the influence of the pressure in the hot water tank while Fig. 5b shows the effects of the ice slurry temperature. In each curve, the starting point of the solid curve is associated with the minimum pressure ratio required by the heat engine to reach operating temperatures. The dotted line represents the physically unavailable zone due to the characteristics of the system. From these figures two main consequences are clear: (a) The use of higher pressures in the hot water tank allows to substantially increase the value of the RTE and the power produced, so the use of pressurized tanks improves the performance of the system, but this feature requires an increase in the investments. In the following analyses, it will be assumed that the water pressure (P_{H2O}) is 0.2 MPa; (b) The effect of ice slurry temperature (T_L) is important since a decrease of the temperature in the cold tank results in a clear increase in both the power output and efficiency.

Fig. 6 summarizes the effects of internal irreversibilities on the overall system using the RTE-power plots. Those effects associated with compression and expansion are shown in Fig. 6a. Note how the isentropic efficiency is the most influential irreversibility parameter in both the RTE and power output. Fig. 6b compares the loop-like behaviors using an expansion valve or a hydraulic expander with the corresponding energy recovery. As expected, the generation of electricity with the expander, which compensates for the energy consumed during compression, improves performance (at a higher cost) but at the expense of a smaller power output. Finally, losses on the overall system due to pressure drops are illustrated in Fig. 6c, which clearly shows that these kinds of irreversibilities are not too significant in the RTE-power performance, at least at low and moderate pressure drops. The effects of the counterflow heat exchanger efficiency are shown in Fig. 7.a. As expected, the effect is clear and follows the same trend that the internal irreversibilities associated with compression or expansion in Fig. 6a.

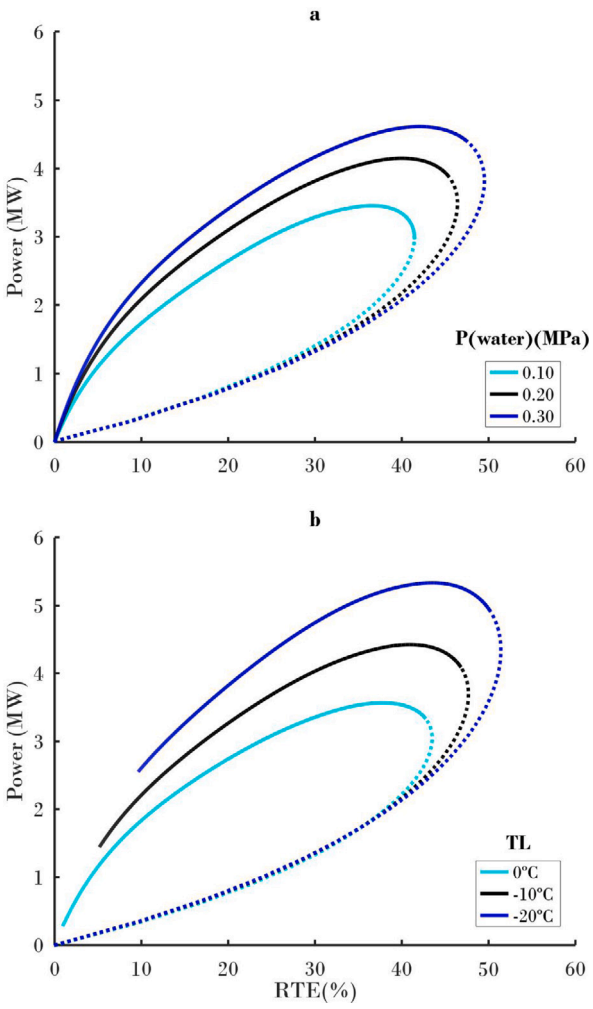

Fig. 5. RTE vs. power loops varying the pressure ratio (r^{HP}). Effect of storage tanks. (a) Hot water tank pressurization in the high temperature zone and (b) ice slurry temperature for a CO_2 working fluid. The baseline arrangement is as in previous figure. The dotted line represents the physically unavailable zones of the loop. Consequently, the power and RTE improves with increasing hot water tank pressure and decreasing ice slurry temperature. As shown in the previous figures, the power and RTE peaks occur at values of r^{HP} between 5 and 7.

4.2. Heat leak effects

One of the advantages of the PHES Rankine systems, especially when CO_2 and hot water are used, is that it operates at lower temperatures than other PHES technologies, and losses to the environment will be lower, allowing the possibility of longer storage periods and thus the long-term storage. Another key advantage in transcritical PHES when the storage fluid is water is that temperatures close to ambient can be reached without crystallization problems, opposite to Brayton PHES arrangement where the crystallization of the storage fluid in the waiting period should be avoided by keeping a high temperature. Concerning the temperature of the cold tank, it is assumed that at least in the short term it remains constant since it is always in the phase change zone and, therefore, the RTE will not be affected by the coupling of the charge and discharge cycles [20].

In Fig. 7.b the RTE-power behaviors are plotted for large variations in the heat leak value. It can seen that the effect is not noticeable, although in the long term it may cause a small drop on the efficiency. So, the long-time heat leaks effects deserve a detailed analysis. The zero-dimensional analysis applied for this calculation was performed with the model developed by Salomone et al. [20] and the properties

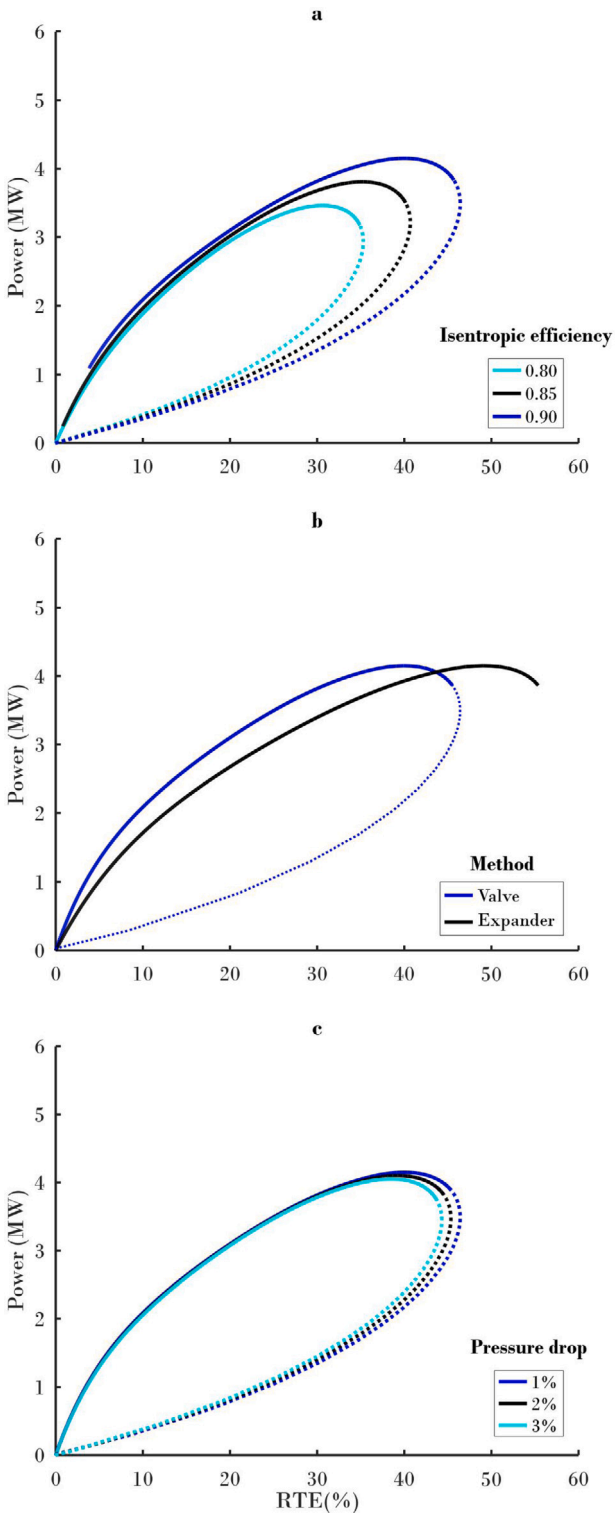

Fig. 6. RTE vs. power loops varying the pressure ratio (r^{HP}). Effect of internal irreversibilities. (a) Isentropic efficiency of compressors, pumps and expanders (turbine and expander), (b) use of valve or expander in charging period (heat pump cycle) and (c) pressure drop for a CO_2 transcritical Rankine cycle. The baseline arrangement and color references are as in previous figures. Accordingly, RTE rises with the increase of isentropic efficiency, with the use of an energy recuperator expander and with the reduction of pressure losses. (For interpretation of the references to color in this figure legend, the reader is referred to the web version of this article.)

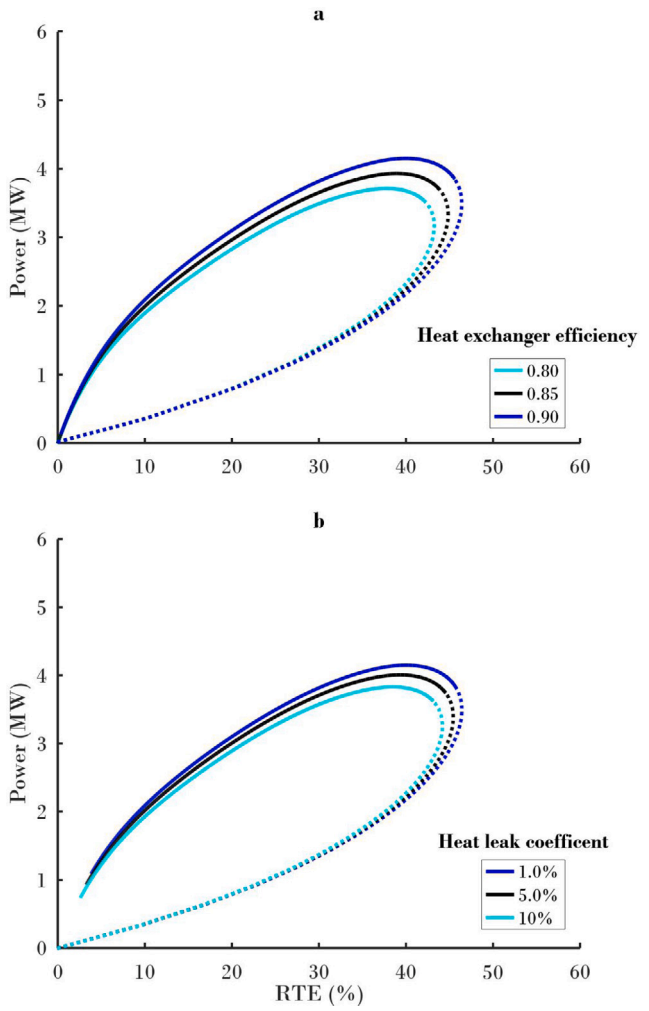

Fig. 7. RTE vs. power loops varying the pressure ratio (r^{HP}). Effect of external irreversibilities for a CO_2 transcritical Rankine system. (a) Effect of heat exchanger efficiency. (b) Effect of heat leak. As expected, heat exchange efficiency and heat leak losses affect negatively the performance. The baseline arrangement is as in previous figures.

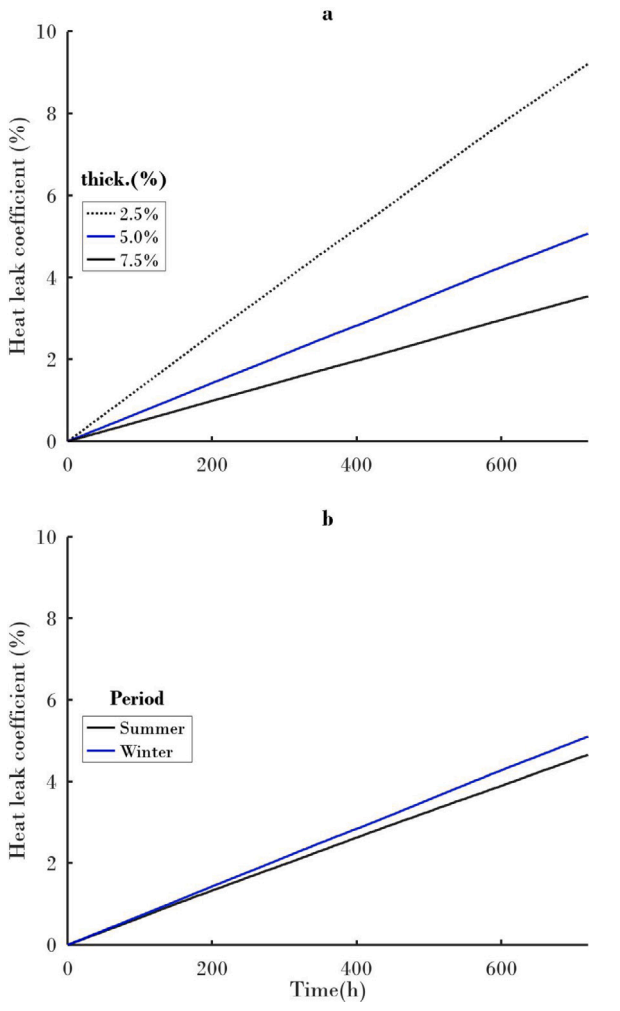

Fig. 8. Heat leak vs time for a pressurized water storage tank of 5MW CO_2 transcritical Rankine plant. (a) Heat leak in winter for a pressurized water tank system evaluated for different glass wool thicknesses and (b) winter–summer comparison for an insulation thickness of 5% of the diameter. Consequently, heat leak losses are reduced as the insulation thickness increases and they are higher in winter than in summer.

of the pressurized water are determined by Coolprop libraries [43]. The impact of this irreversibility is further analyzed considering the tank characteristics for a 5 MW plant using CO_2, hot water and ice slurry as storage media (see Table 2). By evaluating the heat leak of this system over time using a heat transfer model through the tank walls, roof and floor, it is possible to estimate how the loss affects the RTE over time. The variation of the heat leak coefficient for different thicknesses of a mineral wool lining (2.5%, 5.0% and 7.5% of the inside diameter) for the months of winter and a comparison with summer is presented in Fig. 8. It is observed, as expected, that losses decrease with the amount of insulation covering the wall and the heat leak is higher in winter, but its variation will not have a significant effect on the RTE comparing one season with another. The weather significantly influences the performance of the technology for long periods and the thickness of the insulation applied is determinant for this effect. Therefore, it is important to be concerned about the compromise of maintaining storage tanks with the lowest level of losses at the cost of higher insulation costs. In addition, it can be seen that winter and summer weather conditions do not show a significant difference.

Fig. 9 shows the time effect of the temperature of the storage tank that will be used to heat the working gas prior to enter in the turbine. The lower this temperature, the lower the RTE of the system. It can be seen that, for larger thicknesses and long time periods (up to three months) significant drops in temperature are not observed. With insulation of 5% of the diameter, the temperature does not drop more than 5 °C per month. Another detail visible in the graphs is that for short periods the temperature curves can approach a linear behavior.

Table 2
Tank characteristics for Rankine 5 MW system with CO_2 as working fluid, pressurized water and ice slurry (with Height/Length = 0.7 and Height/Max.Level of liquid = 1.1).

m_H (kg/s) = 53.8	M_H (ton) = 968	V_H (m^3) = 969
m_L (kg/s) = 593	M_L (ton) = 10667	V_L (m^3) = 10597
Ice_0 = 30%	$Brine_0$ = 8%	P_{H2O} (MPa) = 0.2

As seen previously in Fig. 7.b, the heat leak does not play a relevant role when the system operates in short cycles of a few hours or days. However, it is vital to maintain a good insulation thickness in the water tank to optimize the system in those situations of long storage periods. The plot in Fig. 10 shows how RTE is affected for three winter months with different insulation thicknesses. It is observed that the decrease is not significant enough when there is a good level of cover walls.

To analyze the influence of size plant on heat losses, simulations were performed for 5, 15 and 25 MW with fixed insulation of 5% of hot tanks. In particular, when heat leaks are evaluated for different plant sizes, see Fig. 11, it is noted how the heat leak coefficient is

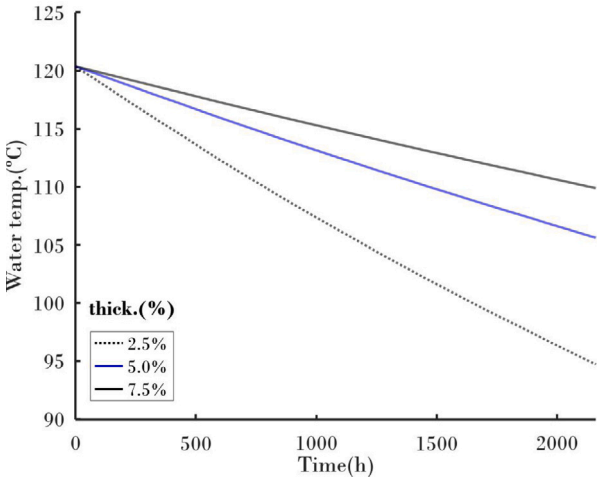

Fig. 9. Pressurized water temperature vs storage time. It is observed that the decrease is smaller with a good insulation thickness.

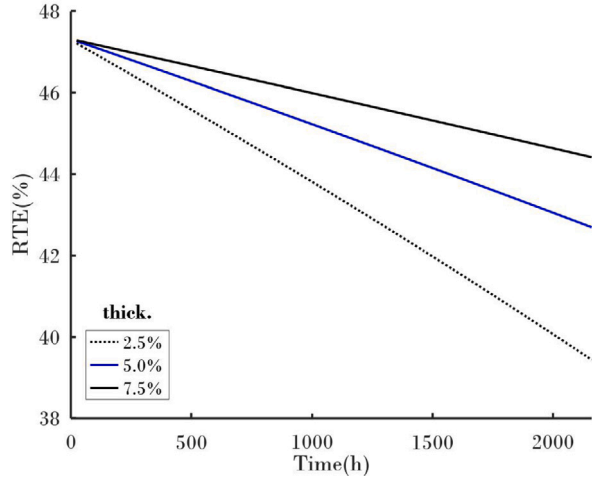

Fig. 10. RTE with storage time for different glass wool thicknesses. Over time the RTE efficiency decreases but the decrease is smaller with a higher level of insulation.

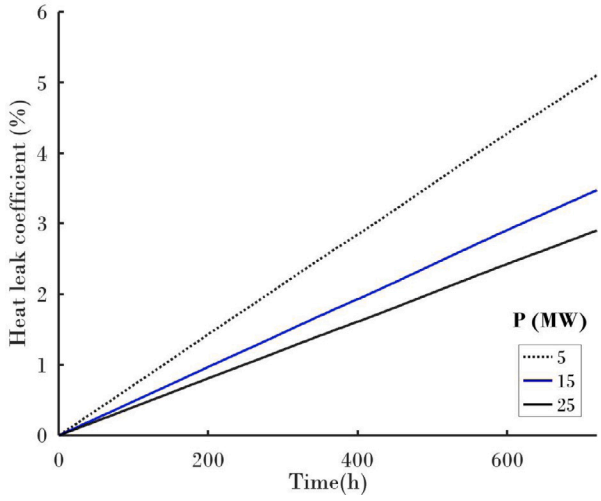

Fig. 11. Heat leak coefficient with storage time for different plant sizes. As plant size increases, the effect of storage time is reduced.

Table 3
Irreversibility parameters for a Rankine 5MW system with CO_2 as working fluid, pressurized water and ice slurry.

$\varepsilon_H^{HP} = 0.95$	$\varepsilon_H^{HE} = 0.95$	$\varepsilon_c = 0.90$	$\varepsilon_b = 0.90$	$\varepsilon_t = 0.90$
$\Delta T_L^{HP} = 5$ °C	$\Delta T_L^{HE} = 5$ °C	$\Delta_{PH} = 1\%$	$\Delta_{PL} = 1\%$	$r^{HP} = 5.5$ $(x = 2)$

Table 4
Temperatures (°C) and pressures (MPa) for the combined Rankine system with CO_2 as working fluid, pressurized water and ice slurry.

$T_1^{HP} = -12$	$T_2^{HP} = 129$	$T_3^{HP} = 23$	$T_4^{HP} = -12$
$T_1^{HE} = 37$	$T_2^{HE} = 115$	$T_3^{HE} = 3$	$T_4^{HE} = -2$
$P_1^{HP} = 2.50$	$P_2^{HP} = 13.75$	$P_3^{HP} = 13.61$	$P_4^{HP} = 2.53$
$P_1^{HE} = 3.37$	$P_2^{HE} = 9.19$	$P_3^{HE} = 9.08$	$P_4^{HE} = 3.33$
$T_{H1} = 120$	$T_{H2} = 17$	$T_L = -7$	$T_0 = 17$

Table 5
Performances results for a Rankine system with CO_2 as working fluid, pressurized water and ice slurry.

$\eta = 12\%$	$COP = 3.23$	$RTE = 47\%$	$m_w = 123$ kg/s	$P = 5$ MW

Table 6
Irreversibility parameters for a Rankine 5MW system with NH_3 as working fluid, thermal oil and ice slurry.

$\varepsilon_H^{HP} = 0.95$	$\varepsilon_H^{HE} = 0.95$	$\varepsilon_c = 0.90$	$\varepsilon_b = 0.90$	$\varepsilon_t = 0.90$
$\Delta T_L^{HP} = 5$ °C	$\Delta T_L^{HE} = 5$ °C	$\Delta_{PH} = 1\%$	$\Delta_{PL} = 1\%$	$r^{HP} = 40$ $(x = 1.5)$

smaller as plant power increases, and thus favor the technology with a lower drop in the energy that can be recovered from the system and the higher RTE. Therefore, it is to be expected that losses from larger plants will have better long-term performances than smaller plants. This trend is due to the improvement in the ratio of the mass contained in the reservoir to the transfer area exposed to the environment.

4.3. Particular configurations

This subsection aims to show two particular configurations with a closer approximation to reality in order to test theoretical predictions. First, the case of a system with carbon dioxide as working fluid and water as storage medium is presented and then, the paper analyzes the case of a system with ammonia, thermal oil and ice slurry with the same power as the previous one.

Table 3 shows the irreversibility parameters selected for the first case, where an expander valve is used.

The numerical results obtained for the temperatures and pressures of each main points of the heat pump and heat engine cycles are shown in Table 4 and plotted on the T–s diagram in Fig. 12. The calculated main performance metrics for the 5MW transcritical CO_2 plant are shown in Table 5. The numerical results, 47% for the RTE, are very valuable and even better than those obtained with Brayton-like systems.

The optimum pressure in the subcooled region depends on the refrigerant properties and operating parameters. In the case of ammonia as the working fluid, the pressures required to reach higher temperatures are lower with respect to CO_2, so the line pressures in the cold region will be lower. However, to reach the critical point, the temperatures are higher than those achievable with water, so the use of a thermal oil will be essential and the pressure ratios are higher.

Now, the NH3 system is addressed. Table 6 shows the irreversibility parameters selected for a Rankine 5 MW system with NH_3 as working fluid and thermal oil using, as before, an expander valve. The results obtained for the temperatures and pressures of each point of the heat pump and heat engine cycles are shown in Table 7 and plotted on the T–s diagram in Fig. 13.

The results in Table 8 show that the efficiencies are higher than in the previous case for the same design power. In addition, when working with lower enthalpy gradients, the working fluid flow is much lower

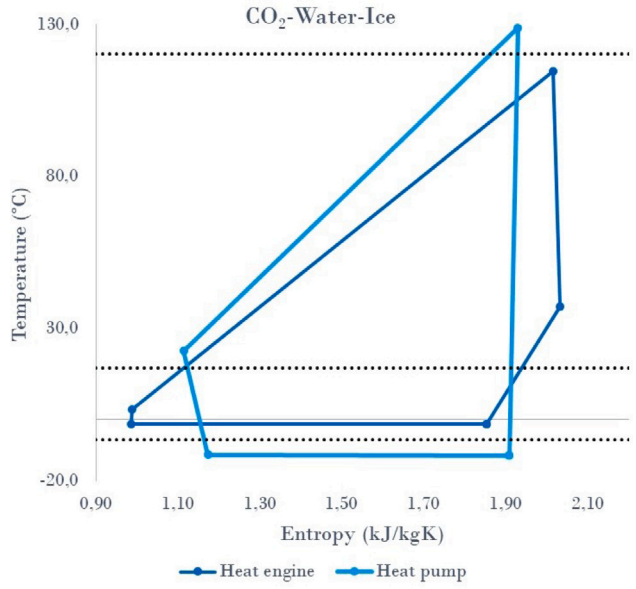

Fig. 12. Heat engine and heat pump T–s plots of the transcritical Rankine with CO_2 as working fluid, pressurized water and ice slurry.

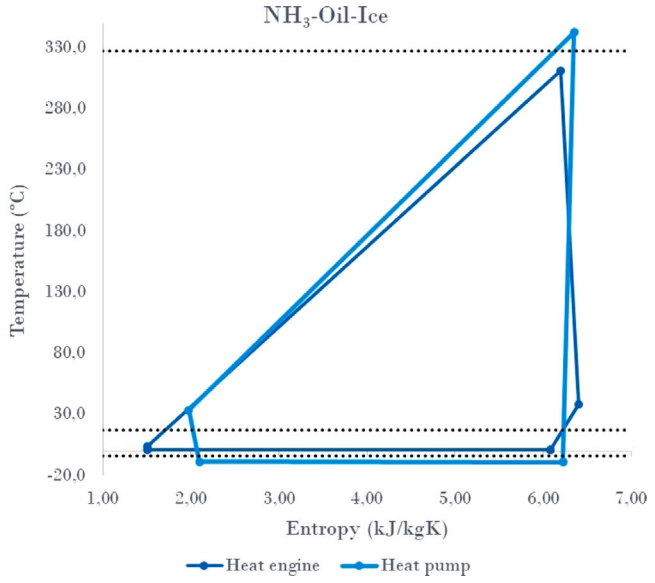

Fig. 13. Heat engine and heat pump T–s plots of the transcritical Rankine with NH_3 as working fluid, thermal oil and ice slurry.

compared to that used with carbon dioxide. However, this system is expected to have higher cost of machines and storage and working fluids.

Two brief comments are in order here. Firstly, The RTE values obtained range between 50% for CO_2 and 70% for NH_3 which surpass those reported by using a Brayton-type system with liquid storage [19,20]. Secondly, in comparison with reported values from Rankine technology the values obtained fit those reported for CO_2 as the working fluid in [32]. Similar values were obtained by Vinnemeier et al. [38] and Ayachi et al. [48].

5. Conclusions

This work presents a general description of the PHES storage technology for a transcritical Rankine model, inspired by the need to regulate the intermittency of renewable sources and to take advantage of surplus energy. The reasons why such an electrical energy storage technology is interesting mainly arise from its promising efficiency, long lifetime and the possibility of locating it anywhere, even next to wind or solar farms.

From the results, it is clear that with increasing temperature and pressure storage in the hot tank and decreasing ice slurry temperature, the round-trip efficiency gradually increases.

The round trip efficiency values obtained are between 50% for CO_2 and 70% for NH_3 and they are clearly higher than those obtained (25%–35%) with Brayton-type system with liquid storage previously developed [19,20]. Main reasons could be greater external losses and heat leaks since Brayton PHES requires higher temperature storage using molten salts instead of water or thermal oils. In addition, storage fluids are more expensive (water is cheaper than molten salts) and have crystallization problems. However, the costs and insecurities of high working pressures to achieve good recovery temperatures mean that Rankine technology needs to be further evaluated, particularly from an economic point of view.

The formation of loop-like behaviors in the RTE vs power plots is primarily due to the peak in heat engine cycle efficiency and the stabilization of COP after a certain level of pressure ratio. It is difficult to make a comparison with other studies performed on the Rankine cycle due to the different theoretical approaches and the lack of prototypes working on this technology, but the results obtained are comparable to those of the model patented by Hemrle and then optimized by Morandin and Mercangoez reaching RTE values between 50 and 60% [32] for CO_2. Similar values were obtained by Ayachi et al. [48],Vinnemeier et al. [38], among other authors. As mentioned above, there is not much experience with ammonia but the results obtained by Koen et al. [29] show efficiencies higher than 50% using ambient temperature in the low pressure zone. Good results, around 50%–70%; when thermal oils are used to store at temperatures higher than pressurized water, they are very similar to those obtained by Zhao et al. [31].

The use of CO_2 as transcritical working fluid and water as a storage medium is promising, but its efficiency is limited by the narrow range of temperatures of the storage medium. Regarding the use of ammonia as working fluid, whose thermal limits are more accessible and with higher RTE, is limited by its toxicity and the high compression ratios required to reach the usual working temperatures of thermal oils, but the efficiencies achieved are much more encouraging.

Concerning with losses, it has been found that those associated to internal irreversibilities coming from compressions and expansions are the most relevant, while heat leak effects are not important for short times. In particular, for a 5 MW plant with CO_2 as working fluid, heat leak coefficient amounts up to 5% after one month changing the RTE by about 0.04% per day for an average thickness of about 5% of the tank diameter. Working with greater insulation thickness and high powers favors the improving of the RTE performance in time.

Table 7
Temperatures (°C) and pressures (MPa) for Rankine system with NH_3 as working fluid, thermal oil and ice slurry.

$T_1^{HP} = -9$	$T_2^{HP} = 343$	$T_3^{HP} = 33$	$T_4^{HP} = -9$
$T_1^{HE} = 38$	$T_2^{HE} = 311$	$T_3^{HE} = 4$	$T_4^{HE} = 1$
$P_1^{HP} = 0.300$	$P_2^{HP} 11.7$	$P_3^{HP} = 11.6$	$P_4^{HP} = 0.303$
$P_1^{HE} = 0.450$	$P_2^{HE} = 11.5$	$P_3^{HE} = 11.6$	$P_4^{HE} = 0.446$
$T_{H1} = 327$	$T_{H2} = 17$	$T_L = -4$	$T_0 = 17$

Table 8
Performances results for the combined Rankine system with NH_3 as working fluid, thermal oil and ice slurry.

$\eta = 28\%$	$COP = 2.44$	$RTE = 70\%$	$m_w = 9.4$ kg/s	$P = 5$ MW

The presented model and simulation work plays an important role to introduce the new concept of Rankine PHES storage systems, gives a comparative thermodynamic analysis and provide a preliminary design of the system. The technology is simple, replicable and provides good efficiency results. If the difficulties regarding high working pressures can be overcome, it could become a promising storage system as a substitute for common batteries.

In a more general context, it is clear that the problems caused by the penetration of renewable energy production at grid-scale applications, mainly due to variable weather conditions, could be properly addressed by the different energy storage technologies. Much of them are commercially available but are non-mature yet. Further and systematic investigation on their durability and reliability are needed. In particular, high-temperature thermal energy storage plays a central role in current renewable energy technologies although more thermo-economical studies complemented with simulation techniques and optimization algorithms are required to fit the better suitability of the working fluids with the phase change materials, molten salts and packed bed materials.

CRediT authorship contribution statement

D. Salomone-González: Conceptualization, Software, Validation, Formal analysis, Writing – original draft, Writing – review & editing. **P.L. Curto-Risso:** Conceptualization, Supervision, Validation, Formal analysis, Writing – original draft, Writing – review & editing, Funding acquisition. **A. Calvo Hernández:** Supervision, Validation, Formal analysis, Writing – original draft, Writing – review & editing. **A. Medina:** Supervision, Validation, Formal analysis, Writing – original draft, Writing – review & editing. **J.M.M. Roco:** Validation, Formal analysis, Writing – original draft, Writing – review & editing. **J. Gonzalez-Ayala:** Validation, Formal analysis, Writing – original draft, Writing – review & editing.

Declaration of competing interest

The authors declare the following financial interests/personal relationships which may be considered as potential competing interests: Pedro L. Curto Risso reports financial support was provided by National Agency for Research and Innovation.

Data availability

Data will be made available on request.

Acknowledgments

Authors acknowledge financial support from Program IA, University of Salamanca (Ref. 18K203), and from Agencia Nacional de Investigación e Innovación (ANII), Spain; Fondo Sectorial de Energía, Uruguay; contract FSE-1-2018-1-153077 and Scholarship program of ANII, Spain POS-NAC-2021-1-169805. J.G.A. also acknowledges financial support from University of Salamanca, with Contract No. 0218 463AB01. We thanks valuable comments and suggestions from a anonymous Referee which greatly improved the final presentation of the paper.

References

[1] K. Attonaty, P. Stouffs, J. Pouvreau, J. Oriol, A. Deydier, Thermodynamic analysis of a 200 MWh electricity storage system based on high temperature thermal energy storage, Energy 172 (2019) 1132–1143.

[2] M. Argyrou, P. Christodoulides, S. Kalogirou, Energy storage for electricity generation and related processes: Technologies appraisal and grid scale applications, Renew. Sustain. Energy Rev. 94 (2018) 804–821, http://dx.doi.org/10.1016/j.rser.2018.06.044.

[3] A. Arabkoohsar, G.B. Andresen, Dynamic energy, exergy and market modeling of a High Temperature Heat and Power Storage System, Energy 126 (2017) 430–443, http://dx.doi.org/10.1016/j.energy.2017.03.065.

[4] Ahmad Arabkoohsar, Combination of air-based high-temperature heat and power storage system with an Organic Rankine Cycle for an improved electricity efficiency, Appl. Therm. Eng. 167 (2019) (2020) 114762, http://dx.doi.org/10.1016/j.applthermaleng.2019.114762.

[5] Ahmad Arabkoohsar, Pumped heat storage system, Mech. Energy Storage Technol. (1147) (2021) 125–14862, http://dx.doi.org/10.1016/B978-0-12-820023-0.00006-7.

[6] Siemens, Siemens siemens industrial decarbonization using electric thermal energy storage (ETES), 2016, https://www.https://www.siemensgamesa.com/en-int/products-and-services/hybrid-and-storage/thermal-energy-storage-with-etes-add.

[7] L. Wan, X. Lin, L. Chai, L. Peng, D. Yu, H. Chen, Cyclic transient behavior of the Joule-Brayton based pumped heat electricity storage: Modeling and analysis, Renew. Sustain. Energy Rev. 111 (2019) 523–534.

[8] T. Desrues, J. Ruer, P. Marty, J.F. Fourmigué, A thermal energy storage process for large scale electric applications, Appl. Therm. Eng. 30 (2010) 425–432.

[9] A.J. White, G. Parks, C.N. Markides, Thermodynamic analysis of pumped thermal electricity storage, Appl. Therm. Eng. 53 (2013) 291–298.

[10] A. White, J. McTigue, C. Markides, Wave propagation and thermodynamic losses in packed-bed thermal reservoirs for energy storage, Appl. Energy 130 (2014) 648–657.

[11] J.D. McTigue, A.J. White, C.N. Markides, Parametric studies and optimisation of pumped thermal electricity storage, Appl. Energy 137 (2015) 800–811.

[12] J.D. McTigue, C.N. Markides, A.J. White, Performance response of packedbed thermal storage to cycle duration perturbations, J. Energy Storage 19 (2018) 379–392.

[13] J. Guo, L. Cai, J. Chen, Y. Zhou, Performance evaluation and parametric choice criteria of a Brayton pumped thermal electricity storage system, Energy 113 (2016) 693–701.

[14] J. Gonzalez-Ayala, D. Salomone-González, A. Medina, J.M.M. Roco, P.L. Curto-Risso, A. Calvo Hernández, Multicriteria optimization of Brayton-like pumped thermal electricity storage with liquid media, J. Energy Storage 44 (2021) 103242, http://dx.doi.org/10.1016/j.est.2021.103242.

[15] C.S. Turchi, J. Vidal, M. Bauer, Molten salt power towers operating at 600–650C: Salt selection and cost benefits, Sol. Energy 164 (March) (2018) 38–46.

[16] The Moonshot Factory, Malta, malta storing renewable energy in molten salt, 2022, https://x.company/projects/malta.

[17] R.B. Laughlin, Pumped thermal grid storage with heat exchange, J. Renew. Sustain. Energy 9 (2017) 1–16.

[18] P. Farres-Antunez, J.D. McTigue, A.J. White, A pumped thermal energy storage cycle with capacity for concentrated solar power integration, in: March Offshore Energy and Storage Summit, OSES, Brest, France, 2019, http://dx.doi.org/10.1109/OSES.2019.8867222.

[19] D. Salomone-Gonzalez, J. Gonzalez-Ayala, A. Medina, J. Roco, P. Curto-Risso, A. Calvo Hernandez, Pumped heat energy storage with liquid media: Thermodynamic assessment by a Brayton-like model, Energy Convers. Manage. 226 (2020) 113540, http://dx.doi.org/10.1016/j.enconman.2020.113540.

[20] D. Salomone-González, P. Curto-Risso, F. Favre, Modeling of heat leak effect in round trip efficiency for Brayton pumped heat energy storage with liquid media, by cooling and heating of the reservoirs tanks, J. Energy Storage 46 (2022) 103793, http://dx.doi.org/10.1016/j.est.2021.103793.

[21] G. Frate, L. Ferrari, U. Desideri, Multi-criteria investigation of a pumped thermal electricity storage (PTES) system with thermal integration and sensible heat storage, Energy Convers. Manage. 208 (2020) 112530, http://dx.doi.org/10.1016/j.enconman.2020.112530.

[22] J. Hemrle, M. Mercangoez, L. Kaufmann, Patent application publication (10) Pub. No.: US 2012/0080168 A1, 2012.

[23] J. Hemrle, M. Mercangoez, L. Kaufmann, Patent application publication (10) Pub. No.: US 2012/0222423 A1, 2012.

[24] M. Morandin, F. Maréchal, F. Buchter, M. Mercangöz, Conceptual design of a thermo-electrical energy storage system based on heat integration of thermodynamic cycles - Part B: Studying alternative system configurations, in: Proceedings of the 24th International Conference on Efficiency, Cost, Optimization, Simulation and Environmental Impact of Energy Systems, ECOS 2011, Vol. 45, 2011, pp. 2497–2511, http://dx.doi.org/10.1016/j.energy.2012.03.033.

[25] M. Morandin, F. Maréchal, M. Mercangöz, F. Buchter, Conceptual design of a thermo-electrical energy storage system based on heat integration of thermodynamic cycles - Part A: Methodology and base case, Energy 45 (2012) 375–385, http://dx.doi.org/10.1016/j.energy.2012.03.031.

[26] M. Morandin, M. Mercangöz, J. Hemrle, F. Maréchal, D. Favrat, Thermoeconomic design optimization of a thermo-electric energy storage system based on transcritical CO2 cycles, Energy 58 (2013) 571–587, http://dx.doi.org/10.1016/j.energy.2013.05.038.

[27] M. Kim, J. Pettersen, C. Bullard, Fundamental process and system design issues in CO2 vapor compression systems, Prog. Energy Combust. Sci. 30 (2004) 119–174.

[28] R. La Fauci, B. Heimbach, E. Kaffe, F. Kienzle, L. Küng, Feasibility Study of an Electrothermal Energy Storage in the City of Zurich, IET Conference Publications, 2013, 2013.

[29] A. Koen, P. Farres-Antunez, White, A study of working fluids for transcritical pumped thermal energy storage cycles, 2019.
[30] M. Abarr, J. Hertzberg, L. Montoya, Pumped Thermal Energy Storage and Bottoming System Part B: Sensitivity analysis and baseline performance, Energy 119 (2017) 601–611.
[31] Y. Zhao, J. Song, M. Liu, Y. Zhao, A.V. Olymmpios, P. Sapin, J. Yan, C. Markides, Thermo-economic assessments of pumped-thermal electricity storage systems employing sensible heat storage materials, Renew. Energy (2022) 431–456, http://dx.doi.org/10.1016/j.renene.2022.01.017.
[32] M. Mercangöz, J. Hemrle, L. Kaufmann, A. Z'Graggen, C. Ohler, Electrothermal energy storage with transcritical CO2 cycles, Energy 45 (2012) 407–415, http://dx.doi.org/10.1016/j.energy.2012.03.013.
[33] A. Olympios, J. McTigue, P. Farres-Antunez, A. Tafone, A. Romagnoli, Y. Li, Y. Ding, W. Steinmann, L. Wang, H. Chen, C. Markides, Progress and prospects of thermo-mechanical energy storage—a critical review, Prog. Energy. 3 (2021) 022001.
[34] H. Yamaguchi, X. Zhang, K. Fujima, M. Enomoto, N. Sawada, Solar energy powered Rankine cycle using supercritical CO2, Appl. Therm. Eng. 26 (2006) 2345–2354.
[35] Y. Chen, W. Pridasawas, P. Lundqvist, Dynamic simulation of a solar-driven carbon dioxide transcritical power system for small scale combined heat and power production, Solar Energy 84 (2010) 1103–1110, http://dx.doi.org/10.1016/j.solener.2010.03.006.
[36] E. Cayer, N. Galanis, M. Desilets, H. Nesreddine, P. Roy, Analysis of a carbon dioxide transcritical power cycle using a low temperature source, Appl. Energy 86 (2009) 1055–1063, http://dx.doi.org/10.1016/j.apenergy.2008.09.018.
[37] R. Cazar, Construcción del diagrama de fases del dióxido de carbono, 2013.
[38] P. Vinnemeier, M. Wirsum, D. Malpiece, R. Bove, Integration of heat pumps into thermal plants for creation of large-scale electricity storage capacities, Appl. Energy 184 (2016) 506–522.
[39] V. Aga, E. Conte, B. Burcker, M. Ramond, R. Carroni, Supercritical CO 2 based heat pump cycle for electrical energy storage for utility scale dispatchable renewable energy power plants GE renewable energy, in: The 5th International Supercritical CO2 Power Cycles Symposium, Vol. 94, 2016.
[40] Y. Hao, Q. He, D. Du, A trans-critical carbon dioxide energy storage system with heat pump to recover stored heat of compression, Renew. Energy 152 (2020) 1099–1108, http://dx.doi.org/10.1016/j.renene.2020.01.099.
[41] B. Knodel, D. France, U. Choi, M. Wambsganss, Heat transfer and pressure drop in ice water slurries, Appl. Therm. Eng. 20 (2000) 671–685.
[42] Melinder, E. Granryd, Using property values of aqueous solutions and ice to estimate ice concentrations and enthalpies of ice slurries, Int. J. Refrig. 28 (2005) 13–19.
[43] I. Bell, W. Jorrit, S. Quolin, V. Lemort, Pure and pseudo-pure fluid thermophysical property evaluation and the open-source thermophysical property library CoolProp, Ind. Eng. Chem. Res. 53 (2014) 2498–2508, http://pubs.acs.org/doi/abs/10.1021/ie4033999.
[44] W. Steinmann, Thermo-mechanical concepts for bulk energy storage, Renew. Sustain. Energy Rev. 75 (2017) 205–219, http://dx.doi.org/10.1016/j.rser.2016.10.065.
[45] S. Kaushik, S. Tyagi, P. Kumar, Finite time thermodynamics of power and refrigeration cycles, 2017, pp. 1–317.
[46] M. Moran, H. Shapiro, Fundamentos de termodinámica básica, 2004, https://www.mendeley.com/library/.
[47] J. Eaton, GNU Octave Manual, Network Theory Limited, 2002.
[48] F. Ayachi, N. Tauveron, T. Tartière, S. Colasson, D. Nguyen, Thermo-Electric Energy Storage involving CO2 transcritical cycles and ground heat storage, Appl. Therm. Eng. 108 (2016) 1418–1428, http://dx.doi.org/10.1016/j.applthermaleng.2016.07.063.